Scanning microscopy using a short-focal-length Fresnel zone plate

Ethan Schonbrun,* Winnie N. Ye, and Kenneth B. Crozier

School of Engineering and Applied Science, Harvard University, Cambridge, Massachusetts 02138, USA
**Corresponding author: schonbru@seas.harvard.edu*

Received March 13, 2009; revised May 31, 2009; accepted June 10, 2009;
posted June 22, 2009 (Doc. ID 108635); published July 14, 2009

We demonstrate a form of scanning microscopy using a short-focal-length Fresnel zone plate and a low-NA relay telescope. Owing to a focal length of only 5 μm, the zone plate produces large wavefront tilt and consequently severe vignetting for off-axis illumination. By scanning an optically trapped fluorescent sphere, we measure the vignetted collection region of the zone-plate imaging system. The fluorescence collection efficiency is sharply peaked and has a lateral width of 550 nm, which agrees with numerical simulations.

OCIS codes: 180.5810, 050.1965, 170.2520, 080.1010.

Both confocal and near-field microscopes use small apertures to restrict light collection to confined regions in the object plane. The spatial resolution of these techniques is limited by the aperture size and the collection efficiency, which affects the signal-to-noise ratio. While both near-field [1] and confocal microscopies [2] have proven to be powerful imaging techniques, each scanning measurement requires precise alignment to a pinhole aperture, making parallelization and integration difficult. Here, we demonstrate a high-resolution scanning microscope where the spatial filter consists of the clear aperture of a relay lens. Interestingly, although the clear aperture of the relay lens has a diameter of approximately 1.27 cm (0.5"), the short focal length of the zone plate results in a submicrometer collection region. In this microscope, a short-focal-length zone plate is scanned over an object, and the light that it collects is imaged onto a detector. This system offers high collection efficiency and high resolution. In this scheme, parallel scanning microscopy using a Fresnel zone-plate array would require only a single spatial filter, rather than an array of pinholes. Fresnel zone plates make ideal integrated lenses, because they are planar and are capable of extremely short focal lengths [3–5]. We anticipate that the enhanced tolerances and simplicity of this scheme will be advantageous in microfluidic and microelectromechanical-based systems (MEMS) (e.g., [6–10]).

Fresnel zone plates are diffractive lenses that can have extremely short focal lengths. A zone plate can be considered to be a thin hologram where the reference wave is a plane wave and the recorded wave has the phase of a spherical wave originating from a point at a focal length away. The complex field of the hologram H is the interference of the reference and recorded wavefronts,

$$H(r) = |1 + \exp(-jk_n\sqrt{r^2+f^2})|^2 = 2 + \exp(jk_n\sqrt{r^2+f^2}) + \exp(-jk_n\sqrt{r^2+f^2}), \quad (1)$$

where r is the radial coordinate, k_n is the wavevector in the focusing medium, and f is the focal length. The continuous valued interference pattern can be encoded into a binary-phase zone plate using a threshold condition. High-NA binary zone plates produce only two focal spots, one at f, the other at $-f$, because higher orders are evanescent. The focal length f can be as short as a few optical wavelengths, or even zero in surface-plasmon structures.

In this Letter, we investigate the collection region of a system consisting of a short-focal-length zone plate and a relay telescope. This corresponds to operating the zone plate in a collection mode, where the zone plate is illuminated by a spherical wave-point source, as shown in Fig. 1. In this case, the amplitude of the spherical wave should not be dropped, as it plays an important role in defining the field U emerging from the zone plate,

$$U = H \times S = [2 + \exp(jk_n\sqrt{r^2+f^2}) + \exp(-jk_n\sqrt{r^2+f^2})] \times \frac{A_0}{\sqrt{r^2+f^2}}\exp(-jk_n\sqrt{r^2+f^2}) = \frac{A_0}{\sqrt{r^2+f^2}} + \ldots, \quad (2)$$

where S is the complex field of a point source and A_0 is its amplitude. As expected, the zone plate collimates the point source by cancelling the spherical

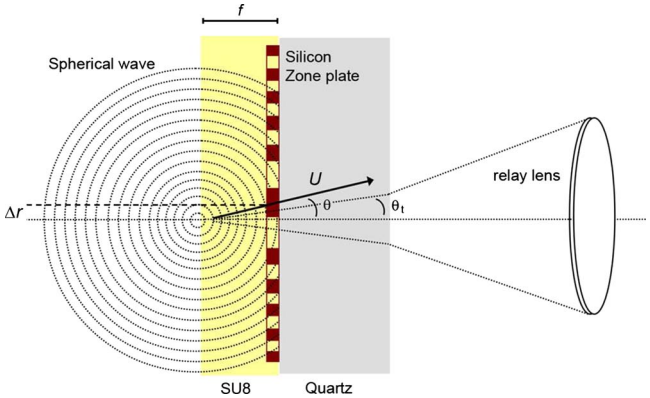

Fig. 1. (Color online) Diagram of the scanning zone-plate imaging system. A point source at an axial distance f, the focal length, illuminates the zone plate. The point source is a transverse distance of Δr from the optical axis, which is shown as a dashed line. A relay lens collects light emerging from the zone plate up to an angle θ_t.

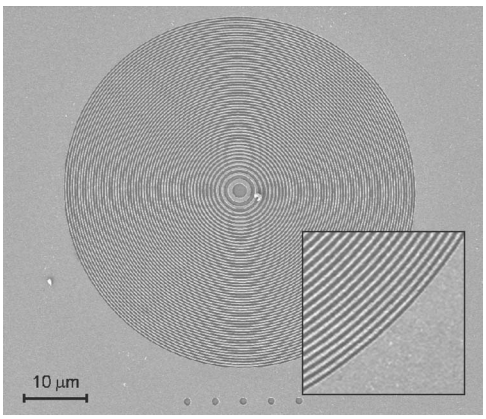

Fig. 2. (Color online) Scanning electron micrograph of the silicon zone plate before coating with the SU8 immersion film.

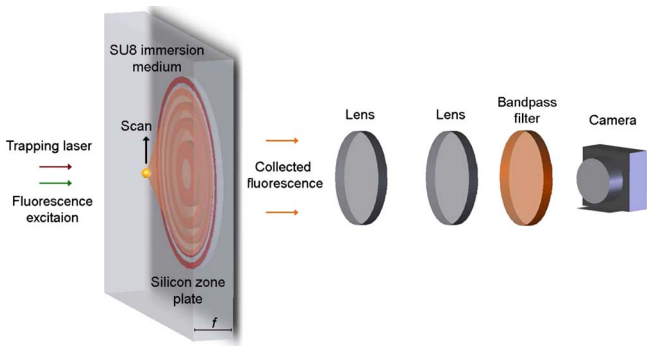

Fig. 4. (Color online) Schematic of the experiment. Polystyrene spheres are trapped in a fluid chamber and scanned across the field of view of the zone plate. Fluorescence collected by the zone plate is imaged through the quartz substrate by relay optics and through a fluorescence emission filter onto a camera.

phase, but the field is not uniform in amplitude, which is analogous to a collection apodization factor [11]. Other interference terms have been dropped from Eq. (2), as noted by the ellipsis. The intensity of the wave emerging from the zone plate $|U|^2$ is Lorentzian and has a FWHM of $2f$. For large-NA zone plates that have an aperture much larger than their focal length, this width can be significantly smaller than their physical aperture.

When the point source is located on the optical axis, the field collimated by the zone plate has a flat phase distribution and consequently no wavefront tilt. A transverse displacement Δr of the point source produces a wavefront tilt with an angle of $\theta = \arctan(\Delta r/f)$. In the zone-plate scanning microscope, the field emerging from the zone-plate aperture is collected by a low-NA telescope that has a maximum collection angle θ_t. When $\theta > \theta_t$, light collected by the zone plate is not captured by the telescope and therefore does not hit the detector. This is an extreme form of vignetting that restricts the zone plate field of view and is enhanced by the zone plate's short focal length [7]. Vignetting occurs when $\Delta r \geqslant f \tan \theta_t$.

To demonstrate this imaging technique, we have fabricated a solid immersion zone plate with an aperture diameter of 50 μm and a focal length of 5 μm. The NA is 1.55, and its maximum focusing cone angle is 78.7°. The zone plate is patterned from a 120 nm amorphous silicon film using electron-beam lithography and reactive ion etching. We then spin coat a 5 μm film of SU8, which acts as the immersion medium and has a refractive index of 1.58 at a wavelength of 575 nm. For a thickness of 120 nm, there is a phase contrast of π between the silicon rings and the open areas, which are filled with SU8. Figure 2 shows a scanning electron micrograph (SEM) of the fabricated zone plate. We measure the transmission coefficient of the silicon film at a wavelength of 575 nm to be 0.26 owing to both absorption and reflection.

We perform a numerical characterization of the vignetted field of view using a nonparaxial scalar beam propagation algorithm (BPA) [12]. In the simulation, a point source is located at a distance of 5 μm, which is equal to the focal length, from the zone plate. The zone plate has a phase step of π and a transmission coefficient of 0.26. The field emerging from the zone plate is then low-pass Fourier filtered up to an angle of θ_t, corresponding to the maximum collection angle of the low-NA telescope, and the resulting intensity distribution is integrated. By translating the point source in the focal plane of the zone plate, we are able to map out the spatially variant collection efficiency of the imaging system. The BPA assumes that the zone plate is a thin element and that the diffraction efficiency is not a function of polarization or radial position. Although for high-NA diffractive elements this has been shown not to be rigorously the case [13], numerical simulations give reasonable agreement to the experimental measurements.

Figure 3(a) shows the intensity collected by the imaging system as a function of the transverse position of the point source, calculated using the BPA. The

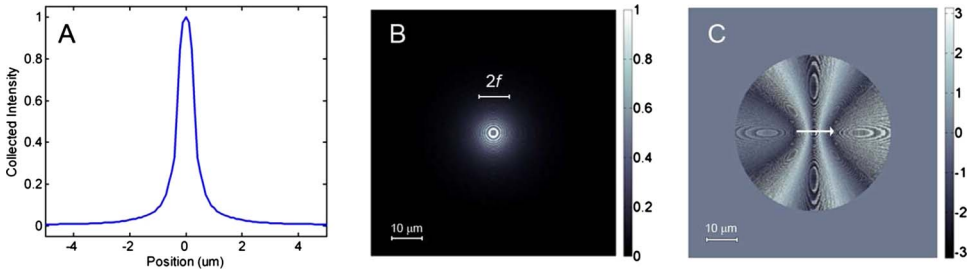

Fig. 3. (Color online) Fourier beam propagation simulations of a 5 μm focal length (f) zone plate. A, Collection efficiency as a function of transverse position for the zone plate and relay lens optical system. B and C, Amplitude and phase, respectively, of the field directly behind the zone plate when the point source is 0.5 μm from the optical axis.

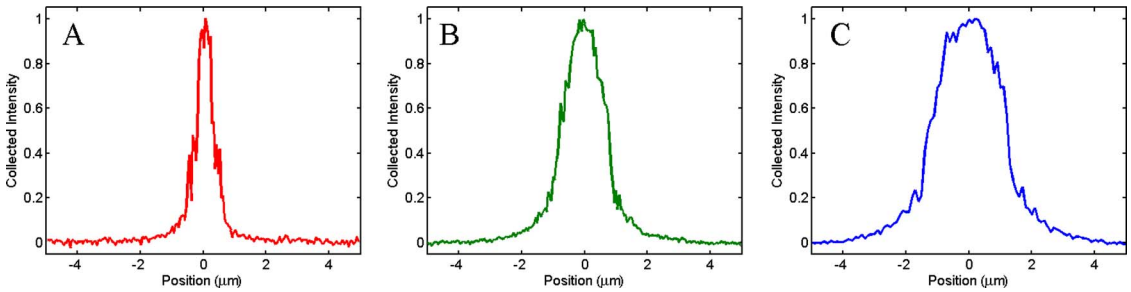

Fig. 5. (Color online) Collected fluorescent signal versus position for sphere scanning experiments. A, B, and C show the scanning of 0.5, 1.1, and 2.0 μm diameter fluorescent spheres, respectively. Raw, unfiltered data is presented. Data are normalized to have a maximum of unity, and background subtraction has been carried out.

collected intensity is a sharply peaked function that reaches its maximum when the point source is aligned to the optical axis of the zone plate. The FWHM of the collection peak is 660 nm when a 0.06 NA telescope is used in the back aperture of the zone plate. Figures 3(b) and 3(c) show the amplitude and phase, respectively, of the field directly behind the zone plate when the point source is offset from the optical axis by 0.5 μm. The phase of the field exhibits the predicted wavefront tilt, where the direction is shown by the white arrow, which is responsible for shifting the beam out of the aperture of the relay lens.

To experimentally characterize the microscope, we scan fluorescent spheres of different sizes across the field of view. The spheres are first optically trapped and pinned against the SU8/water interface using a counterpropagating IR laser with a free-space wavelength of 976 nm. After the sphere is pinned to the SU8 surface, the substrate is scanned by a piezo motor, as shown in Fig. 4. When the sphere is centered directly over the zone plate, the collection efficiency reaches a maximum. As the sphere is scanned away from the zone-plate center, the collection efficiency quickly decreases and consequently maps out the vignetted field of view. The back aperture of the zone plate is imaged with unity magnification using a two-lens telescope onto a CCD camera. The lenses have focal lengths of 100 mm and diameters of 2.54 cm (1"). The clear-aperture diameter of these relay lenses is estimated to be approximately 1.27 cm (0.5") owing to occlusion of the mount, giving an NA of 0.063. The CCD pixel values over the area of the zone plate are then integrated to give the total collection signal.

Figure 5 shows the collected fluorescence as a function of position for spheres with diameters of 0.5, 1.1, and 2.0 μm that have manufacturer-specified coefficients of variation of 4.7%. The piezo motor takes 30 nm discrete steps and is operated at a velocity of 50 steps/s. Frames are captured by the CCD camera at 30 Hz, resulting in a displacement of 50 nm between successive frames. Brownian motion of the trapped spheres results in a 25 nm standard deviation of their position. From Fig. 5, the FWHM of the line scans of the 0.5, 1.1, and 2 μm spheres, are 0.546 ± 0.038 μm, 1.320 ± 0.115 μm, and 1.970 ± 0.088 μm, respectively. The 0.5 μm sphere acts approximately like a point source, and the FWHM of the scan agrees reasonably well with the numerically computed scan in Fig. 3(a).

In this Letter, we have presented a new scanning microscopy technique based on enhanced vignetting of a short-focal-length Fresnel zone plate. This method is capable of high resolution and high light-collection efficiency. The optical resolution is determined by both the magnitude of the wavefront tilt and the width of the Lorentzian-shaped intensity distribution at the aperture of the relay lens. By reducing the relay lens aperture, we can further increase the resolution, which will be the subject of future work. We believe this microscope will be valuable in microfluidic and MEMS systems because of the zone plate's compact size, high resolution, and high collection efficiency.

This work was supported by the Defense Advanced Research Projects Agency (DARPA) and the National Science Foundation (NSF). We also thank the reviewers for insightful commentary.

References

1. E. Betzig and J. K. Trautman, Science **257**, 189 (1992).
2. W. J. Denk, D. W. Piston, and W. W. Webb, *Handbook of Biological Confocal Microscopy*, J. B. Pawley, ed. (Plenum, 1995).
3. D. Gil, R. Menon, and H. I. Smith, J. Vac. Sci. Technol. B **21**, 2956 (2003).
4. R. Brunner, M. Burkhardt, A. Pesch, O. Sandfuchs, M. Ferstl, S. Hohng, and J. O. White, J. Opt. Soc. Am. A **21**, 1186 (2004).
5. E. Schonbrun and K. B. Crozier, Opt. Lett. **33**, 2017 (2008).
6. D. L. Dickensheets and G. S. Kino, Opt. Lett. **21**, 764 (1996).
7. H. J. Tiziani, R. Achi, R. N. Kramer, and L. Wiegers, Appl. Opt. **35**, 120 (1996).
8. D. Gil, R. Menon, D. J. D. Carter, and H. I. Smith, J. Vac. Sci. Technol. B **18**, 2881 (2000).
9. X. Heng, D. Erickson, L. R. Baugh, Z. Yaqoob, P. W. Sternberg, D. Psaltis, and C. Yang, Lab Chip **6**, 1274 (2006).
10. P. M. Lundquist, C. F. Zhong, P. Zhao, A. B. Tomaney, P. S. Peluso, J. Dixon, B. Bettman, Y. Lacroix, D. P. Kwo, E. McCullough, M. Maxham, K. Hester, P. McNitt, D. M. Grey, C. Henriquez, M. Foquet, S. W. Turner, and D. Zaccarin, Opt. Lett. **33**, 1026 (2008).
11. T. D. Visser, G. J. Brakenhoff, and F. C. A. Groen, Optik **87**, 39 (1991).
12. J. W. Goodman, *Introduction to Fourier Optics* (McGraw-Hill, 1996).
13. N. Davidson and N. Bokor, Opt. Lett. **29**, 1318 (2004).